

Cleveland State University  
EngagedScholarship@CSU



Mechanical Engineering Faculty Publications

Mechanical Engineering Department

10-1-2013


# On the Uniqueness and Sensitivity of Indentation Testing of Isotropic Materials

J. K. Phadikar  
*University of Delaware*

T. A. Bogetti  
*U.S. Army Research Laboratory*

Anette M. Karlsson  
*Cleveland State University, a.karlsson@csuohio.edu*

Follow this and additional works at: [https://engagedscholarship.csuohio.edu/enme\\_facpub](https://engagedscholarship.csuohio.edu/enme_facpub)

 Part of the [Materials Science and Engineering Commons](#), and the [Mechanical Engineering Commons](#)

**How does access to this work benefit you? Let us know!**

*Publisher's Statement*

NOTICE: this is the author's version of a work that was accepted for publication in International Journal of Solids and Structures. Changes resulting from the publishing process, such as peer review, editing, corrections, structural formatting, and other quality control mechanisms may not be reflected in this document. Changes may have been made to this work since it was submitted for publication. A definitive version was subsequently published in International Journal of Solids and Structures, 50, 20-21, (10-01-2013); 10.1016/j.ijsolstr.2013.05.028

## Original Citation

Phadikar, J. K., Bogetti, T. A., and Karlsson, A. M., 2013, "On the Uniqueness and Sensitivity of Indentation Testing of Isotropic Materials," International Journal of Solids and Structures, 50(20-21) pp. 3242-3253.

This Article is brought to you for free and open access by the Mechanical Engineering Department at EngagedScholarship@CSU. It has been accepted for inclusion in Mechanical Engineering Faculty Publications by an authorized administrator of EngagedScholarship@CSU. For more information, please contact [library.es@csuohio.edu](mailto:library.es@csuohio.edu).

# On the uniqueness and sensitivity of indentation testing of isotropic materials

J.K. Phadikar<sup>a</sup>, T.A. Bogetti<sup>b</sup>, A.M. Karlsson<sup>a,c,\*</sup>

<sup>a</sup> Department of Mechanical Engineering, University of Delaware, Newark, DE, United States

<sup>b</sup> U.S. Army Research Laboratory, Aberdeen Proving Ground, MD, United States

<sup>c</sup> Fenn College of Engineering, Cleveland State University, Cleveland, OH, United States

## 1. Introduction

Instrumented indentation is widely used to probe the elastic and plastic material properties of engineering materials (Cheng and Cheng, 2004; Oliver and Pharr, 1992; Johnson, 1987; Yan et al., 2007a,b). During the experiment (Fig. 1a), a rigid indenter is pushed into and then removed from the surface of a homogeneous solid, while the indentation force,  $P$ , and depth of penetration,  $h$ , are continuously recorded during loading and unloading. The resulting force–displacement relationship (Fig. 1b) is implicitly related to the material properties and the geometry of the solid and the indenter. The objective of an indentation analysis is to correlate the force–displacement response to the material properties of the solid, such that the elastoplastic properties can be determined from an indentation experiment. However, various authors (Cheng and Cheng, 1999; Capehart and Cheng, 2003; Tho et al., 2004; Alkorta et al., 2005) have shown that several materials can result in indistinguishable force–displacement relationships. Thus, a one-to-one relationship between material properties and experimentally obtained data is not guaranteed. In addition, it is important to investigate the sensitivity for experimental errors of the

technique: will a small experimental error result in a reliable solution? In the present work, a systematic investigation of these two issues is conducted for conical indentation on an infinite half-space.

A review of the essential concepts involved in indentation analysis is presented below to serve as foundation for the present work.

### 1.1. Shape functions

We consider a homogeneous, isotropic material with linear-elastic response, followed by power-law strain hardening plasticity. The power-law for strain-hardening (Fig. 2) provides a very good description of the behavior of many metals or metallic alloys (Dieter, 1976; Lubliner, 1990). According to this, the uniaxial stress–strain relationship of a material can be expressed as:

$$\sigma = \begin{cases} E\varepsilon & \text{for } \varepsilon \leq \frac{Y}{E} \\ K\varepsilon^n & \text{for } \varepsilon \geq \frac{Y}{E} \end{cases} \quad (1)$$

Here,  $\sigma$  and  $\varepsilon$  correspond to the stress and the strain, respectively and  $E$ ,  $Y$  and  $n$  denote the elastic modulus, the yield strength and the strain hardening exponent of the material, respectively.  $K$  is a strength coefficient which can be written as  $K = E^n Y^{1-n}$ . Poisson's ratio is assumed constant since it is a minor factor in indentation (Cheng and Cheng, 2004). Thus, changing this will not result

\* Corresponding author at: Fenn College of Engineering, Cleveland State University, Cleveland, OH, United States. Tel.: +1 216 687 2558; fax: +1 216 687 9280.  
E-mail addresses: a.karlsson@csuohio.edu, karlsson@udel.edu (A.M. Karlsson).

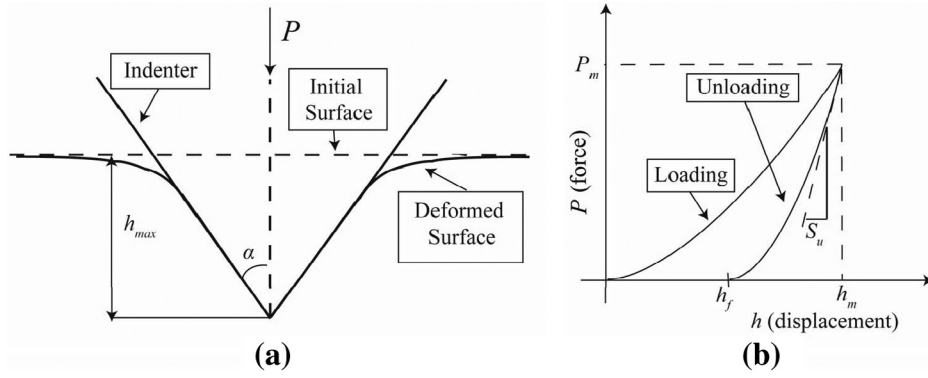


**Fig. 1.** Schematic diagram of (a) conical indentation on half-space and (b) the typical force–displacement response obtained during loading and unloading.

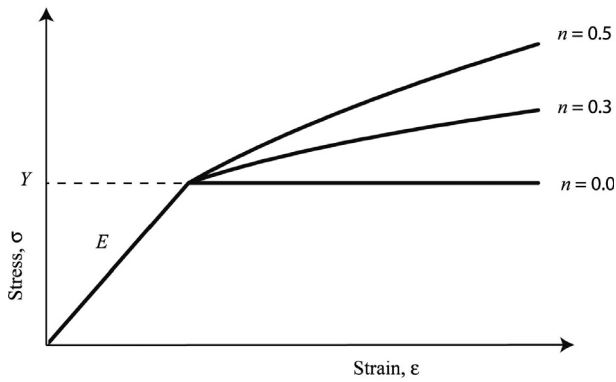


**Fig. 2.** Schematic stress–strain relationship of an elastic, power, law hardening material.

in considerable deviation in monitored indentation parameters. In all, the material parameter set to be determined in the indentation analysis is  $(E, Y, n)$ .

The concept of representative stress,  $\sigma_r$ , and representative strain,  $\varepsilon_r$ , have been used to simplify the functional equations arising from indentation analyses (Yan et al., 2007a, 2007b; Dao et al., 2003; Cao and Lu, 2004a,b; Ogasawara et al., 2009; Cao et al., 2005; Cao and Huber, 2006). In such indentation analyses,  $\varepsilon_r$  is identified and the set  $(E, \sigma_r, n)$  is determined from the indentation analysis. In turn,  $Y$  is determined using the obtained  $\varepsilon_r$ ,  $E$ ,  $\sigma_r$  and  $n$ . Thus, the two sets of unknown parameters,  $(E, Y, n)$  and  $(E, \sigma_r, n)$ , are fundamentally equivalent and the use of representative stress and strain does not reduce the number of unknowns. Since one can use either  $(E, Y, n)$  or  $(E, \sigma_r, n)$  as the unknown parameter set, we will here use the set  $(E, Y, n)$ .

The most widely used indenter geometry, conical indenter, will be considered (Fig. 1a) in this work. A conical indenter can be characterized by the half-angle,  $\alpha$ . The Berkovich indenter can be represented with a conical indenter of  $\alpha = 70.3^\circ$  (Cheng and Cheng, 2004; Lichinchi et al., 1998).

The force–displacement response (Fig. 1b) obtained from a displacement controlled (maximum indentation depth,  $h_m$ ) indentation experiment can be characterized by various “shape functions” such as the total energy during loading (e.g. the area under the loading curve),  $W_t$ , maximum force,  $P_m$ , unloading slope,  $S_u$ , elastic energy (e.g. the area under the unloading curve),  $W_e$ , and residual or final depth,  $h_f$  (Yan et al., 2007a, 2007b; Dao et al., 2003; Ogasawara et al., 2009; Cao et al., 2005). The force–displacement relationship depends on the material properties, such as  $E$ ,  $Y$  and  $n$ ,

and geometrical parameters, such as  $h_m$  and  $\alpha$ . The shape functions,  $\Pi_i$  can be written as:

$$\Pi_i = \mathcal{F}_i(E, Y, n, \alpha, h_m); \quad i = 1 - 5 \quad (2)$$

where  $\Pi_1 = W_t$ ,  $\Pi_2 = P_m$ ,  $\Pi_3 = S_u$ ,  $\Pi_4 = W_e$  and  $\Pi_5 = h_f$ . Using the above relations, various combinations of the shape functions can also be expressed in terms of the material and geometric parameters, for example,

$$\begin{aligned} W_t/h_f &= \mathcal{F}_6(E, Y, n, \alpha, h_m); \quad S_u/W_e = \mathcal{F}_7(E, Y, n, \alpha, h_m); \\ W_t/W_e &= \mathcal{F}_8(E, Y, n, \alpha, h_m); \quad S_u/h_f = \mathcal{F}_9(E, Y, n, \alpha, h_m) \end{aligned} \quad (3)$$

Applying dimensional analysis and Buckingham’s PI theorem (Buckingham, 1914) to Eq. (2), the relations can be simplified as follows:

$$\Psi_i = \bar{\mathcal{F}}_i\left(\frac{E}{Y}, n, \alpha\right); \quad i = 1 - 5 \quad (4)$$

where  $\Psi_1 = \frac{W_t}{Yh_m^2}$ ,  $\Psi_2 = \frac{P_m}{Yh_m}$ ,  $\Psi_3 = \frac{S_u}{Yh_m}$ ,  $\Psi_4 = \frac{W_e}{Yh_m^2}$ ,  $\Psi_5 = \frac{h_f}{h_m}$  and the over-head bar indicates normalized form.

In an indentation experiment, the geometrical parameters are known. Thus, for fixed geometric parameters ( $\alpha$  and  $h_m$ ), Eqs. (2) and (4) can be written as

$$\begin{aligned} \Pi_i &= \mathcal{G}_i(E, Y, n) \\ \Psi_i &= \bar{\mathcal{G}}_i\left(\frac{E}{Y}, n\right); \quad i = 1 - 5 \end{aligned} \quad (5)$$

In summary, the shape functions are characteristic functions that describe the indentation response. The functions  $\mathcal{G}_i$  and  $\bar{\mathcal{G}}_i$  can be determined by extensive finite element analysis where the indentations are simulated and the material parameters are varied systematically. To this end, finite element models simulating the indentation experiment are built and the shape functions are extracted from the force–displacement response for the range of material properties investigated. With the functional forms established, Eq. (5) serves as the constitutive relationship between the data obtained from a real indentation test (e.g.  $W_t$ ) and the properties sought ( $E$ ,  $Y$  and  $n$ ). This is further explored in Section 1.2.

### 1.2. Uniqueness and sensitivity

Since three unknown material properties ( $E$ ,  $Y$ ,  $n$ ) are to be determined to define our material, any three shape functions (or their combinations) can be selected to establish the properties. However, only two of the five equations involving shape functions are independent, see for example (Cheng and Cheng, 1999; Capehart and Cheng, 2003; Tho et al., 2004; Alkorta et al., 2005). That is, two different materials can give an identical

**Table 1**

Various shape functions and half-angles used by previous researchers for dual indentation technique.

Shape function combination	Ref.
$S_u _{70.3^\circ} P_m _{70.3^\circ} P_m _{45^\circ}$	Le (2008)
$S_u _{70.3^\circ} h_f _{70.3^\circ} P_m _{70.3^\circ} P_m _{60^\circ}$	Chollacoop et al. (2003)
$(S_u/P_m) _{70.3^\circ} P_m _{70.3^\circ} P_m _{60^\circ}$ and $(W_t/W_e) _{70.3^\circ} P_m _{70.3^\circ} (W_t/W_e) _{60^\circ}$	Lan and Venkatesh (2007)
$S _{70.3^\circ} (P_m/S) _{70.3^\circ} (P_m/S) _{80.5^\circ}$	Wang et al. (2005)
$(W_e/W_t) _{60^\circ} P_m _{60^\circ} (W_e/W_t) _{70.3^\circ} P_m _{70.3^\circ}$	Swaddiwudhipong et al. (2005)
$S _{70.3^\circ} h_f _{70.3^\circ} P_m _{70.3^\circ} P_m _{60^\circ} 50^\circ 42.3^\circ$	Bucaille et al. (2003)
Two of $P_m _{60^\circ} P_m _{63.14^\circ} P_m _{70.3^\circ}$ ( $E$ was known)	Yan et al. (2007a,b)
$S_u _{70.3^\circ} P_m _{70.3^\circ} P_m _{60^\circ}$	Heinrich et al. (2009)
$(W_t/W_e) _{70.3^\circ} P_m _{70.3^\circ} (W_t/W_e) _{60^\circ}$	Le (2009, 2011)

force–displacement response and therefore identical shape functions. It follows that a single indentation cannot uniquely determine the three unknown material properties of a substrate.

To address this shortcoming of the single indentation technique, dual indentation techniques have been proposed by several authors (Table 1). In dual indentation techniques, two indenter geometries are utilized giving two additional shape functions. Since only three equations are needed, the premise is that two sets of geometrical parameters will provide distinct displacement responses, thus it will be possible to uniquely determine the material properties. For two sets of fixed geometrical parameters ( $\alpha = \alpha_1, h_m = h_{m1}$  and  $\alpha = \alpha_2, h_m = h_{m2}$ ), Eqs. (2) and (4) can be written as:

$$\Pi_i^j = \bar{C}_i^j(E, Y, n) \quad (6)$$

$$\Psi_i^j = \bar{C}_i^j \left( \frac{E}{Y}, n \right) \quad ; \quad i = 4 - 5, j = 1, 2$$

where superscripts  $j = 1$  and  $2$  correspond to test 1 and test 2, respectively, and  $i$  is defined after Eqs. (2) and (4). In a dual indentation technique three equations from Eq. (6) are selected, along with two half-angles,  $\alpha_1$  and  $\alpha_2$ . Thus, there are innumerable ways to conduct and evaluate a dual indentation experiment.

However, Chen et al. (2007) showed that certain groups of materials exist which result in indistinguishable force–displacement responses for dual indentation testing. The authors showed that generally materials with low values of  $E/Y$  and  $n$  fall into this category. The range of such materials depends on the half-angles of the indenters used in the dual indentation experiment. For example, the authors reported that for dual indentation with  $\alpha_1 = 70.3^\circ$  and  $\alpha_2 = 80^\circ$ , materials with identical force–displacement relationships lie in the range of  $100 < E/Y < 250$  and  $0.0 < n < 0.2$ . Thus, unfortunately a dual indentation technique does not guarantee a unique data reduction scheme for all materials.

Closely related to uniqueness is sensitivity to experimental errors (Chollacoop et al., 2003; Lan and Venkatesh, 2007; Le, 2008; Hyun et al., 2011; Cao and Lu, 2004a,b; Swaddiwudhipong et al., 2005). A complete and systematic investigation of the sensitivity to experimental error in dual indentation techniques has not been developed and is the focus of the present work.

In the following section the procedure to develop the functional forms of Eqs. (3) and (4) will be described. With that established, we introduce the concept of condition number to capture uniqueness and sensitivity. Finally, sensitivity analysis results for a wide range of dual indentation techniques and material properties will be presented to evaluate their reliability.

## 2. Functional forms from finite element analysis

In this section, the finite element model and regression analysis used to derive the functional forms of Eqs. (2)–(4) will be described.

### 2.1. Finite element model

Finite element simulations were performed using the commercial finite element program ABAQUS (ABAQUS, 2009). The flat half-space is assumed to be composed of homogeneous, isotropic, linear-elastic, power-law strain-hardening material, Eq. (1). An axisymmetric, two-dimensional model was adopted and approximately 25,000 CAX4R elements were used to model the half-space. The mesh is significantly refined in the vicinity of indentation to resolve the stress and strain field. The conical indenter is modeled as a rigid body. Coulomb's friction law is used and the friction coefficient between the surfaces is taken to be 0.15 (Bowden and Tabor, 2001). Several simulations with refined meshes and time increments were investigated for the convergence study. The model used in the investigation was one that gave the same results as a finer mesh and time increment. Thus, the selected refinement was demonstrated to be sufficient to accurately capture the mechanism of indentation. The surface nodes of the half-space were traction free and the nodes along the axis of symmetry were constrained in the direction normal to indenter displacement to simulate symmetry conditions. The bottom of the half-space was kept fixed in all three directions.

The model simulates the rigid indenter being pushed into the half-space to a predefined displacement,  $h_m$ , and then the indenter is removed. The reaction force as a function of indenter displacement is recorded continuously over the loading and unloading sequence, similar to a real indentation experiment (Fig. 1b).

### 2.2. Functional forms

To develop the functional forms presented in Eqs. (2)–(4), a material set with elastic modulus  $80 \leq E$  (GPa)  $\leq 300$  and yield stress  $0.1 \leq Y$  (GPa)  $\leq 2.0$  was chosen to cover a wide range of  $E/Y$  ratios ( $80 \leq E/Y \leq 1000$ ). We limit the investigations to this range since it was shown by Chen et al. (2007) that materials with identical force–displacement relationships have comparatively lower  $E/Y$  ratios and as will be discussed later, non-uniqueness can be considered as an “extreme case of sensitivity.” The strain hardening exponent was taken to be  $0.0 \leq n \leq 0.5$ , which is common for metals (Chen et al., 2007). Poisson's ratio was taken to be constant at 0.3. As previously noted, Poisson's ratio has only a minor effect on the force–displacement response. Various half-angles ranging from  $50^\circ$  to  $85^\circ$  were used in the study. Altogether, approximately 400 finite element simulations were conducted to attain the functional forms. Considering Eqs. (5) and (6), the normalized shape functions of the left hand sides were expressed as functions of  $E/Y$  and  $n$  for fixed values of  $\alpha$ . The fitting function used has the following form:

$$f\left(\frac{E}{Y}, n\right) = \sum_{i=0}^5 \sum_{j=0}^5 \left( \bar{C}_{ij} \left( \frac{E}{Y} \right)^i n^j \right) \quad (7)$$

Here,  $\bar{C}_{ij}$  are fitting coefficients.<sup>1</sup>

The initial unloading slope,  $S_u$ , was computed using the two points associated with the maximum load and 90% of the maximum load (i.e. 10% of the unloading curve). For a  $50^\circ$  half-angle conical indenter penetrating a half-space, the fitting coefficients for the normalized unloading slope,  $S_u$ , are tabulated in Table 2, as an example of how this fitting routine is implemented. Fitting coefficients for other cases are not presented in this paper for

<sup>1</sup> In this case, 36 coefficients are needed to describe the functions. This may seem like a large number of parameters, and we note that we are **not** striving to develop a relationship where the parameters can be interpreted as physical parameters, but we are just interested in finding “fitting parameters” that describe the intricate response. This method is commonly adopted in reverse analysis, see for example (Cao and Lu, 2004a,b; Chen et al., 2006; Hyun et al., 2011; Le, 2008).

**Table 2**Fitting coefficients for Eq. (7) for the unloading slope,  $S_u$ , for  $\alpha = 50^\circ$ .

$\eta_{ij}$	$j = 0$	$j = 1$	$j = 2$	$j = 3$	$j = 4$	$j = 5$
$i = 0$	-1.3776E-08	1.8984E-08	-9.4536E-09	2.0161E-09	-1.5497E-10	-8.5559E-14
$i = 1$	3.6781E-05	-5.0824E-05	2.5416E-05	-5.4501E-06	4.2205E-07	1.3196E-10
$i = 2$	-3.6636E-01	5.0698E-02	-2.5452E-02	5.4923E-03	-4.2953E-04	5.1739E-08
$i = 3$	1.6313E01	-2.2605E01	1.1411E01	-2.4864	1.9758E-01	-1.8699E-04
$i = 4$	-2.4736E03	3.5185E04	-1.8409E03	4.1875E02	-3.6111E01	3.1671
$i = 5$	8.8827E04	-1.3523E05	7.6600E04	-1.8983E04	1.7449E03	-2.5036E01

brevity.

### 3. Sensitivity and uniqueness

In this section, a method will be developed to determine  $E$ ,  $Y$  and  $n$  of a material based on a conical dual indentation test. The uniqueness and sensitivity of the solution will be discussed in a manner similar to the examples given in Appendix A.

#### 3.1. Method of iso- $P_m/(S_u h_m)$ lines

For conical indentation on a half-space, only two of the five shape functions listed in Eq. (2) are independent (Alkorta et al., 2005). Consider two shape functions: maximum load,  $P_m$ , and unloading slope,  $S_u$ . For a single indentation test, two materials (materials 1 and 2) will have identical force–displacement relationships if both of them have the same values of  $P_m$  and  $S_u$ . That also holds if they have the same  $P_m$  and the same  $P_m/S_u$ . Thus, two conditions for identical force–displacement relationship can be written as:

$$(P_m)_1 = (P_m)_2 \quad (8a) \leftarrow$$

$$(P_m/S_u)_1 = (P_m/S_u)_2 \quad (8b) \leftarrow$$

Using the relation of normalized  $P_m$  in Eq. (4), the first condition can be written as:

$$Y_1 h_m^2 \bar{G}_2 \left( \frac{F_1}{Y_1}, n_1 \right) = Y_2 h_m^2 \bar{G}_2 \left( \frac{E_2}{Y_2}, n_2 \right) \quad (9)$$

which gives the ratio of their yield strengths as follows:

$$r = \frac{Y_1}{Y_2} = \bar{G}_2 \left( \left( \frac{F_1}{Y_1} \right)_2, n_2 \right) / \bar{G}_2 \left( \left( \frac{E}{Y} \right)_1, n_1 \right) \quad (10)$$

The two materials can be made to satisfy the second condition, Eq. (8b) by deriving non-dimensional relations involving  $P_m$  and  $S_u$  in Eq. (4), which gives

$$\frac{P_m}{S_u h_m} = \bar{G}_2 \left( \frac{F}{Y}, n \right) / \bar{G}_3 \left( \frac{E}{Y}, n \right) = \bar{G}_6 \left( \frac{E}{Y}, n \right) \quad (11)$$

Eq. (8b) can be rewritten using Eq. (11) as:

$$\bar{G}_6 \left( \left( \frac{F}{Y} \right)_1, n_1 \right) = \bar{G}_6 \left( \left( \frac{E}{Y} \right)_2, n_2 \right) \quad (12)$$

The graph of Eq. (11) for  $\alpha = 50^\circ$  with  $P_m/(S_u h_m)$  as a function of  $E/Y$  and  $n$  is shown in Fig. 3. Iso- $P_m/(S_u h_m)$  lines can be drawn in the  $E/Y - n$  space which is shown in Fig. 4a. Since all materials lying on a particular iso- $P_m/(S_u h_m)$  line have identical value of  $P_m/(S_u h_m)$ , it follows that any two materials selected from a particular iso- $P_m/(S_u h_m)$  line will satisfy the second condition for identical force–displacement relationship, Eq. (12). From Fig. 4a, pairs of materials having identical force–displacement relationship can be found in the following steps:

**Step 1:** Select any two points on a particular iso- $P_m/(S_u h_m)$  curve (as illustrated in Fig. 4a). This will give  $(E/Y)$  and  $n$  of two materials

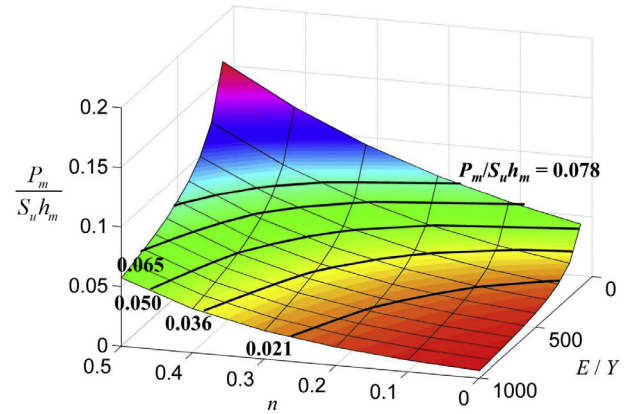


Fig. 3. Graph of the function,  $\frac{P_m}{S_u h_m} = \bar{G}_6 \left( \frac{E}{Y}, n \right)$  (Eq. (11)) for  $\alpha = 50^\circ$ .

that satisfy the second condition of identical force–displacement relationship (Eq. (8b)).

**Step 2:** Determine the ratio  $r = Y_1/Y_2$  from Eq. (10) using  $(E/Y)_1$ ,  $n_1$ ,  $(E/Y)_2$  and  $n_2$  obtained in Step 1. Since Eq. (10) is derived from Eq. (8a), the materials now satisfy the first condition (Eq. (8a)) as well.

**Step 3:** Assume any value of  $Y_2$  and determine  $Y_1$  using  $Y_1 = rY_2$ , from Step 2.

**Step 4:** Using  $Y_1$  and  $Y_2$ , and  $(E/Y)_1$  and  $(E/Y)_2$  obtained in Step 1, determine  $E_1$  and  $E_2$ .

Since  $Y_2$  is selected arbitrarily, there are an infinite number of materials having the same force–displacement relationship corresponding to any two points of an iso- $P_m/(S_u h_m)$  line.

Let us now consider the case of dual indentation testing, for example when  $\alpha = 50^\circ$  (conical indentation) is augmented with three alternative indentation shapes:  $\alpha = 80^\circ$ ,  $70^\circ$  and  $60^\circ$ . Using the same approach discussed above for these three indenters, the iso-lines can be generated. These are shown in Fig. 4b–d respectively together with the iso-lines from  $\alpha = 50^\circ$ . The iso-lines can be used to determine the material properties of a material based on a dual indentation test using the procedure described as follows (described for  $\alpha_1 = 50^\circ$  and  $\alpha_2 = 80^\circ$ ): conduct the dual indentation test with  $\alpha_1 = 50^\circ$  and  $\alpha_2 = 80^\circ$ . Obtain the force–displacement relationships and thereby the quantities  $P_m/S_u h_m$  from the tests corresponding to each half-angle. Draw the two particular iso-lines corresponding to the two half-angles in the  $E/Y - n$  space. Since both the iso-lines correspond to the same material, the intersection of the two lines will give  $E/Y$  and  $n$  for the material. The modulus,  $E$  can be determined using the commonly used “Oliver–Pharr method” (Oliver and Pharr, 1992).

#### 3.2. Demonstration of sensitivity

The basic definitions of condition number and how it can be used to quantify uniqueness and sensitivity are described in Appendix A. A condition number gives a measure of the ratio of perturbation in the solution (e.g., material properties) and pertur-

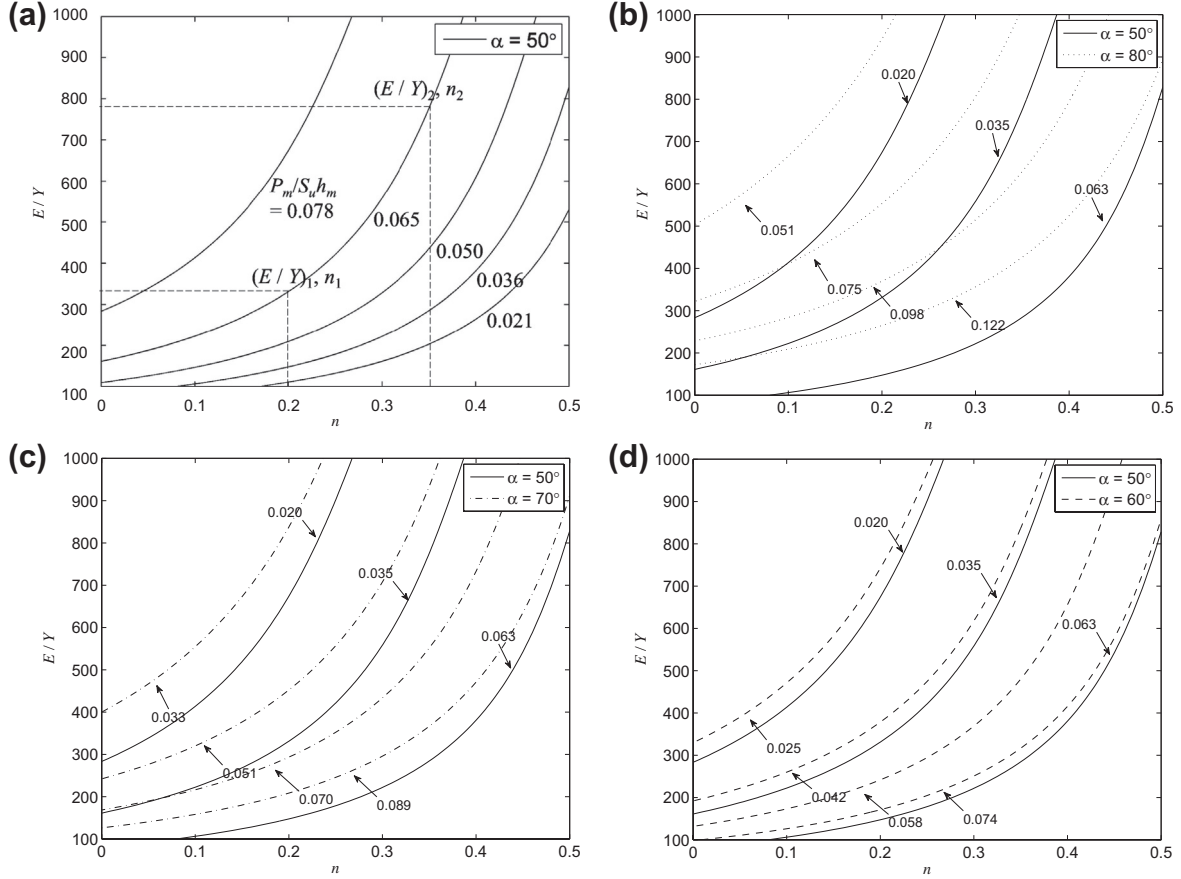


**Fig. 4.** Iso- $(P_m/S_u h_m)$  lines for (a)  $\alpha = 50^\circ$ ; (b)  $\alpha = 50^\circ$  and  $\alpha = 80^\circ$ ; (c)  $\alpha = 50^\circ$  and  $\alpha = 70^\circ$ ; (d)  $\alpha = 50^\circ$  and  $\alpha = 60^\circ$ . As the iso-lines from two tests approach each other, the system becomes increasingly sensitive to experimental errors.

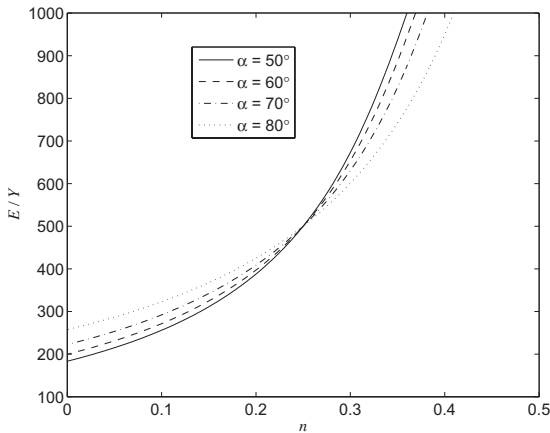


**Fig. 5.** Iso- $(P_m/S_u h_m)$  lines passing through the point  $E/Y = 500$ ,  $n = 0.25$  for four selected conical indenters.

bation in the data (e.g., experimentally obtained indentation shape functions). If the condition number is large, a small perturbation in the data will cause a large change in the solution (i.e., the system is highly sensitive) and vice versa. When the condition number is infinite, several solutions can be found for a given set of data, i.e. the system yields non-unique solutions.

The method of iso- $P_m(S_u h_m)$  lines can be used to assess the sensitivity of dual indentation techniques, that is, assessing how sensitive the technique is to experimental errors. Fig. 4b–d can be compared with Fig. A1a–c. Here  $E/Y$  and  $n$  are equivalent to

the elements of  $\mathbf{x}$  (solution), and values of  $P_m/(S_u h_m)$  corresponding to two different indentation tests are equivalent to the elements of  $\mathbf{y}$  (data) in Appendix A. The sensitivity of the solution (i.e., sensitive to experimental errors) and the condition number of the system increase as the iso-lines get closer to each other, similar to the discussion in Appendix A. For clarity, Fig. 5 illustrates this, where the iso-lines passing through the point  $E/Y = 500$ ,  $n = 0.25$  corresponding to four indenter-tip angles are shown.

Although, condition numbers are not explicitly computed for the examples presented in this section, it can be understood from the discussion in Appendix A that as the indentation system becomes increasingly sensitive and approaches non-uniqueness, the condition number of the system will increase. This will be discussed next in more detail.

#### 4. Condition numbers of single and dual indentation techniques

So far, the issues of sensitivity and non-uniqueness have only been discussed in qualitative terms. We will now attempt to quantify them using the concept of condition numbers.

##### 4.1. Modified condition number

Appendix A gives a brief overview of the definition and establishment of the condition number. The definition of relative error used to define the condition number, is not suitable for indentation problems due to the large differences in numerical values of the elastic modulus,  $E$ , yield strength,  $Y$ , and strain hardening exponent,  $n$ . Thus, we will introduce a new definition of condition num-

ber which measures the relative change as  $\|\Delta \mathbf{z}\|/\|\mathbf{z}\|$  where the definition of the “./” operation is

$$\begin{aligned} \mathbf{m}./\mathbf{n} &= (m_1, m_2, m_3 \dots m_k) ./ (n_1, n_2, n_3 \dots n_k) \\ &= (m_1/n_1, m_2/n_2, m_3/n_3 \dots m_k/n_k) \end{aligned} \quad (13)$$

In this operation, the relative change is measured on an element by element basis. Considering the equation  $\mathbf{y} = \mathbf{f}(\mathbf{x})$ , where,  $x$  denotes the material property vector<sup>2</sup> or a point in the input space,  $\mathbf{x} = (E, Y, n)$ , and  $\mathbf{y}$  denotes the vector of shape functions or a point in the output space,  $\mathbf{y} = (\text{shape functions})$ , similar to Eq. (A1), the modified condition number can be defined as

$$\kappa_m = 1/w(\mathbf{f}, C, \mathbf{z}) \quad (14a)$$

where

$$\begin{aligned} w(\mathbf{f}, C, \mathbf{z}) &= \sup_{\mathbf{x} \text{ in } C} \{t \text{ in } [0, \infty); \|\mathbf{f}(\mathbf{x}) - \mathbf{f}(\mathbf{z})\| ./ \|\mathbf{f}(\mathbf{z})\| \\ &\leq t \|\mathbf{x} - \mathbf{z}\| ./ \|\mathbf{z}\|\} \end{aligned} \quad (14b)$$

and  $\mathbf{z}$  is the point in material space where the condition number is computed,  $C$  is a user-defined domain enclosing  $\mathbf{z}$ . A small  $\kappa_m$  implies that the relative error of the material properties,  $\|\Delta \mathbf{x}\|/\|\mathbf{x}\|$ , is small for a given error in shape functions,  $\|\Delta \mathbf{y}\|/\|\mathbf{y}\|$ , and vice versa: From Eq. (14a), a small  $\kappa_m$  implies large  $w(\mathbf{f}, C, \mathbf{z})$ . Note that in Eq. (14b),  $\|\Delta \mathbf{x}\|/\|\mathbf{x}\|$  is denoted as  $\|\mathbf{x} - \mathbf{z}\|/\|\mathbf{z}\|$  and  $\|\Delta \mathbf{y}\|/\|\mathbf{y}\|$  is denoted as  $\|\mathbf{f}(\mathbf{x}) - \mathbf{f}(\mathbf{z})\|/\|\mathbf{f}(\mathbf{z})\|$ . From Eq. (14b),  $w(\mathbf{f}, C, \mathbf{z})$  approximately denotes the maximum value of  $\|\Delta \mathbf{y}\|/\|\mathbf{y}\|/\|\Delta \mathbf{x}\|/\|\mathbf{x}\|$ . Thus, for a given  $\|\Delta \mathbf{y}\|/\|\mathbf{y}\|$ , a large  $w(\mathbf{f}, C, \mathbf{z})$  implies a small  $\|\Delta \mathbf{x}\|/\|\mathbf{x}\|$ . It follows that a small  $\kappa_m$  results in small  $\|\Delta \mathbf{x}\|/\|\mathbf{x}\|$  for a given  $\|\Delta \mathbf{y}\|/\|\mathbf{y}\|$ . Since  $\kappa_m$  measures the relative change as  $\|\Delta \mathbf{z}\|/\|\mathbf{z}\|$ , it is able to accommodate large numerical differences among the values of  $E$ ,  $Y$  and  $n$ . Well-conditioned systems have condition numbers close to 1, which is the case of tensile testing.

#### 4.2. Computational procedure

To quantify the sensitivity of indentation techniques, the modified condition number,  $\kappa_m$ , has been computed numerically for a range of indentation conditions. The origin of the input space is set at  $\mathbf{z} = (E_0, Y_0, n_0)$ , and the origin of the output space is assumed as the point which is exactly mapped from  $(E_0, Y_0, n_0)$ . The perturbation region or the subdomain,  $C$ , has been selected as:

$$C = \{0.9z_i < z_i < 1.1z_i; i = 1 - 3; \mathbf{z} = (z_1, z_2, z_3)\}$$

Using the functional equations, the region of the output space which corresponds to the perturbation region of input space is determined. For all points in the perturbation region of the input space, the relative differences (Eq. (13)) between the points and the origins are computed. The ratio of the relative differences in output and input region gives the parameter  $t$  of Eq. (14b) at all points of the perturbation region. The maximum value of parameter  $t$  is  $w(\mathbf{f}, C, \mathbf{z})$ . Its reciprocal,  $\kappa_m$  (Eq. (14a)) is the condition number.

For both single and dual indentation and for a given geometry, the condition number is dependent on the material properties (elastic modulus,  $E$ , yield strength,  $Y$ , and strain hardening exponent,  $n$ ). Dimensional analysis shows that the condition number only depends on  $E/Y$  and  $n$ . Thus, denoting the functional relation by  $J$ ,

$$\kappa_m = J\left(\frac{E}{Y}, n\right) \quad (15)$$

For a given indentation geometry, the condition numbers have been calculated at 45 points of the  $E/Y - n$  space, numerically, with

<sup>2</sup> The material properties that are used in this expression are the original properties used in the FE model, and not the ones that are obtained from reverse analysis.

**Table 3**

Condition numbers for single indentation technique for various combinations of shape functions.

Combination of shape function	$\kappa_m^{avg}$
$S_u, W_e, h_f$	88.6
$P_m, W_e, h_f$	131
$P_m, S_u, h_f$	125
$P_m, S_u, W_e$	99.8
$W_t, W_e, h_f$	109
$W_t, S_u, h_f$	106
$W_t, S_u, W_e$	88.6
$W_t, P_m, h_f$	445
$W_t, P_m, W_e$	153
$W_t, P_m, S_u$	165

$E_0/Y_0 = 100, 200, 300, 400, 500, 600, 700, 800, 900$  and  $n_0 = 0.05, 0.15, 0.25, 0.35, 0.45$ . The average condition number for a particular indentation geometry is determined from these 45 cases, and used as the condition number for the indentation geometry,  $\kappa_m^{avg}$ .

#### 4.3. Condition numbers for single indentation

As previously discussed, there are sets of materials resulting in identical force–displacement relationships for the single indentation technique. Thus, the condition number for the single indentation technique should be infinite since it is a non-unique system (Datta, 2010). To investigate this, we computed the average modified condition number,  $\kappa_m^{avg}$ , for conical indentation with  $\alpha = 70^\circ$ . The resulting condition numbers are tabulated in Table 3. Recall that well-conditioned systems have a condition number close to 1. It can be seen that the condition numbers are quite large but finite. The condition numbers are finite since the force–displacement relationships are not truly non-unique, but there are very small differences among the force–displacement relationships of different materials (Tho et al., 2004; Alkorta et al., 2005). These differences are typically indistinguishable with the resolution of a graph when the force–displacement relationships are plotted. Consequently, a finite but very large condition number is obtained for the single indentation test.

#### 4.4. Condition numbers for dual indentation

Next, we consider the condition number for dual indentation. The half-angles of the two indenters are denoted by  $\alpha_1$  and  $\alpha_2$ , where  $\alpha_1 < \alpha_2$ . One can select any two of the five shape functions from an indenter with half-angle  $\alpha_1$  and any one from the indenter with half-angle  $\alpha_2$ . Alternatively, one shape function from indenter with half-angle  $\alpha_1$  and two shape functions from indenter with half-angle  $\alpha_2$  can be used.

First, condition numbers will be presented for a range of shape function combinations and then for various half-angles. The condition numbers were computed for indenters with  $\alpha_1 = 50^\circ$  and  $\alpha_2 = 80^\circ$ . These half-angles may be considered as the limits of the range of half-angles that are of practical use. Results will be presented for the case where two shape functions are selected from  $\alpha_1$  and one shape function is selected from  $\alpha_2$ . Results for the combination of one shape function from  $\alpha_1$  and two shape functions from  $\alpha_2$  are omitted for brevity, since these gave almost the same condition number (for example, selecting  $S_u$  and  $W_e$  from  $\alpha_1 = 50^\circ$  and  $W_t$  from  $\alpha_2 = 80^\circ$  gave almost same results as selection of  $W_t$  from  $\alpha_1 = 50^\circ$  and  $S_u$  and  $W_e$  from  $\alpha_2 = 80^\circ$ ). The condition numbers for 50 combinations of shape functions were arranged in ascending order and are listed in Table 4 (only selected values are tabulated for brevity). The condition numbers range from 5.82 to 322. Small

**Table 4**  
Condition numbers for selected combinations of shape functions of dual indentation. Superscripts 1 and 2 indicate shape functions for half-angles  $\alpha_1$  and  $\alpha_2$  respectively.

Combination #	Shape function combination	$K_m^{avg}$
1	$W_e^2, S_u^1, W_e^1$	5.82
2	$W_e^2, P_m^1, W_e^1$	5.86
3	$W_e^2, W_t^1, W_e^1$	5.87
4	$W_e^2, P_m^1, S_u^1$	7.68
5	$W_e^2, W_t^1, S_u^1$	7.75
6	$P_m^2, P_m^1, S_u^1$	11.7
7	$P_m^2, W_t^1, S_u^1$	11.7
8	$W_t^2, P_m^1, S_u^1$	11.8
9	$W_t^2, W_t^1, S_u^1$	11.8
10	$P_m^2, S_u^1, W_e^1$	12.1
:	:	:
22	$S_u^2, W_t^1, h_f^1$	39.9
23	$S_u^2, P_m^1, h_f^1$	40.6
24	$h_f^2, S_u^1, W_e^1$	42.7
25	$S_u^2, W_t^1, P_m^1$	42.8
26	$h_f^2, W_t^1, S_u^1$	53.5
27	$h_f^2, P_m^1, S_u^1$	54.6
:	:	:
45	$W_e^2, W_t^1, P_m^1$	179
46	$h_f^2, P_m^1, h_f^1$	183
47	$h_f^2, W_e^1, h_f^1$	194
48	$W_t^2, W_t^1, P_m^1$	292
49	$P_m^2, W_t^1, P_m^1$	312
50	$h_f^2, W_t^1, P_m^1$	322

**Table 5**  
Condition numbers for various choices of half-angles for the shape function combination ( $W_e^2, S_u^1, W_e^1$ ).

$\alpha_1$	$\alpha_2$	$K_m^{avg}$
50°	80°	5.62
60°	80°	7.17
50°	70°	9.45
70°	80°	10.7
60°	70°	15.8
50°	60°	16.6

differences in condition number between two combinations may be due to inaccuracy of regression. Thus, for small differences, no conclusions can be drawn about the effectiveness of the combinations involved. Interestingly, many combinations of shape functions for dual indentation yield condition numbers which are of the same order of magnitude as for the single indentation technique. Only a few combinations have condition numbers less than 10. Thus, we conclude that while dual indentation techniques may be inherently more reliable than single indentation techniques, the reliability strongly depends on the shape functions that are chosen.

To investigate the effect the half-angle has on the sensitivity, we considered four half-angles: 50°, 60°, 70° and 80°. The shape function combination giving lowest condition number is  $W_e^2, S_u^1, W_e^1$  (Table 4). Thus, for various choices of  $\alpha_1$  and  $\alpha_2$  among the four angles, condition numbers were computed for the shape function combination  $W_e^2, S_u^1, W_e^1$  and are tabulated in Table 5. It can be seen from Table 5 that as the difference between half-angle increases, the condition number decreases (for example a 50°–80° combination has lower condition number than a 50°–60° combination). It follows that a larger difference between the half-angles results in a less sensitive indentation technique for experimental errors and thus would be a preferred technique. This was observed for

a few cases by Cao and Lu (2004b) and Chen et al. (2007). Further, for a given difference between two half-angles, the sensitivity of the system decreases as the smaller angle increases (Table 5). This was also been observed by Cao and Lu (2004b).

## 5. Sensitivity analysis

As discussed above, the condition number quantifies the sensitivity of indentation testing to experimental error. However, the condition number does not give information about the amount of error that can occur in determined material properties for given experimental error in shape functions. Therefore, we will explore numerical sensitivity analyses to elucidate the characteristics of dual indentation techniques.

The numerical sensitivity analyses are conducted as follows. The material properties are first determined via the (numerically) correct shape functions. These will be denoted by  $E^{ts}$ ,  $Y^{ts}$  and  $n^{ts}$ , where superscript *ts* indicates the true solution. Next, the shape functions are slightly perturbed, simulating an experimental error. Based on these perturbed shape functions, material properties are determined,  $E^{ps}$ ,  $Y^{ps}$  and  $n^{ps}$ , where subscript *ps* indicates the perturbed solution. Thus,  $E^{ps}$ ,  $Y^{ps}$  and  $n^{ps}$  correspond to the properties that would be determined based on an experiment that includes some specific experimental errors. The quantity,  $\delta_{mp}$ , gives a measure in the difference between the true and perturbed solutions (material properties) and is determined by:

$$\delta_{mp} = \sqrt{\left(\frac{E^{ts} - E^{ps}}{E^{ts}}\right)^2 + \left(\frac{Y^{ts} - Y^{ps}}{Y^{ts}}\right)^2 + \left(\frac{n^{ts} - n^{ps}}{n^{ts}}\right)^2} \quad (16)$$

In a well-conditioned system, a small perturbation (small experimental error) does not have a significant effect on the calculated material properties. Thus, a well-condition problem yields a small  $\delta_{mp}$ .

There are several methods used in the literature to conduct numerical sensitivity analyses. A popular method is the so called “one factor at a time” (One Factor scheme) (Chollacoop et al., 2003; Lan and Venkatesh, 2007; Le, 2008; Heinrich et al., 2009). In this case, one shape function is varied while the two others are kept constant. However, errors may occur in all the shape functions simultaneously in a real experiment. Thus, the One Factor scheme may not accurately capture the errors that may occur in a real experiment. In an alternative scheme (Hyun et al., 2011; Heinrich et al., 2009) all shape functions are increased or decreased uniformly by same percentage amount (Uniform Factors scheme). However, as with the One Factor scheme, this scheme does not realistically represents errors as they occur in a real experiment since it is unlikely that all measured data contain the same amount of error. A more effective sensitivity analysis scheme is to vary all shape functions simultaneously by different amounts but keeping all of them within in a fixed limit (Cao and Lu, 2004a; Heinrich et al., 2009; Le, 2009; Le, 2011; Swaddiwudhipong et al., 2005). This is known as a Monte Carlo type sensitivity analysis scheme.

Examples of common sources of errors in indentation experiments are the measured indenter deformation (Cheng and Cheng, 2004), indenter tip roundness (Cheng and Cheng, 2004), substrate surface roughness (Kim et al., 2007) and size effect (increase in hardness at shallow indentation depths) arising from increase in the density of dislocations (Huang et al., 2006). These errors can affect either or both the loading and the unloading response. Thus, the shape functions are subjected to multiple sources of experimental errors. Experimental errors in the shape functions from indentation testing have been reported to be within 5.1% (Wang et al., 2005; Chollacoop et al., 2003). We will investigate sensitivity for three error ranges of  $\pm 1\%$ ,  $\pm 5\%$  and  $\pm 10\%$  with step size of 0.5%, 2.5% and 5% respectively. For example, for the 5% error range, the



**Table 6**

Errors in calculated material properties based on Monte Carlo, One Factor and Uniform Factors sensitivity analyses for dual indentation with  $\alpha_1 = 50^\circ$  and  $\alpha_2 = 80^\circ$  and shape function combination ( $W_e^2, S_u^1, W_e^1$ ),  $\kappa_m^{avg} = 5.8248$ .

Material properties	Percentage error in determined material properties								
	Monte Carlo				One Factor			Uniform Factors	
	0%	$\pm 1\%$ (1, -1, 1)	$\pm 5\%$ (-5, 2.5, 5)	$\pm 10\%$ (-5, 10, -10)	(10, 0, 0)	(0, 10, 0)	(0, 0, 10)	(10, 10, 10)	(-10, -10, -10)
$E$	-0.152	-1.40	8.96	-6.27	-1.32	1.09	9.94	9.83	-10.1
$Y$	0.727	4.67	-45.7	-54.6	24.7	-13.1	0.616	10.8	-9.35
$n$	-0.735	-4.51	41.9	50.7	-17.9	15.3	1.48	-0.735	-0.734

**Table 7**

Errors in calculated material properties based on Monte Carlo sensitivity analysis for dual indentation with  $\alpha_1 = 50^\circ$  and  $\alpha_2 = 80^\circ$  and shape function combination ( $h_f^2, S_u^1, W_e^1$ ),  $\kappa_m^{avg} = 42.715$  and ( $h_f^2, W_t^1, P_m^1$ ),  $\kappa_m^{avg} = 322.06$ .

Material Properties	Percentage error in determined material properties							
	$(h_f^2, S_u^1, W_e^1), \kappa_m^{avg} = 42.715$				$(h_f^2, W_t^1, P_m^1), \kappa_m^{avg} = 322.06$			
	0%	$\pm 1\%$ (-1, -1, 1)	$\pm 5\%$ (-5, 5, 5)	$\pm 10\%$ (-10, 5, 5)	0%	$\pm 1\%$ (1, -0.5, 1)	$\pm 5\%$ (0, 2.5, 5)	$\pm 10\%$ (-10, 5, 10)
$E$	-0.050	-1.75	-2.79	1.67	-7.27	37.4	73.4	-35.1
$Y$	-1.27	49.6	181	189	-33.3	158	155	183
$n$	0.800	-34.2	-99.2	-99.9	32.0	-100	-100	-88.7

three shape functions are perturbed with 5 errors i.e.  $-5\%$ ,  $-2.5\%$ ,  $0\%$ ,  $2.5\%$  and  $5\%$  to give a total of 125 possible combinations. Hence, in the following, the employment of the Monte Carlo analysis is more extensive than in the previous studies (Cao and Lu, 2004a; Heinrich et al., 2009; Le, 2009; Le, 2011; Swaddiwudhipong et al., 2005). A perturbation of 5%, 2.5% and 0% error in the three selected shape functions respectively, will be denoted as (5, 2.5, 0). The procedure for the sensitivity analysis is:

**Step 1:** Consider a specific material (material properties denoted by  $E^{ts}$ ,  $Y^{ts}$  and  $n^{ts}$ ).

**Step 2:** Conduct numerical dual indentation tests with selected combinations of half-angles,  $\alpha$ , and extract the shape functions to obtain numerically correct shape functions.

**Step 3:** Use the concept of reverse analysis outlined in Section 1.3 and the algorithm outlined in Appendix B to determine the material properties using the shape functions obtained in the previous step. This gives the material properties based on the reverse analysis.

**Step 4:** Impose a perturbation on the shape functions from step 2, simulating the experimental error. Compute the material properties  $E^{ps}$ ,  $Y^{ps}$  and  $n^{ps}$  for all perturbations combinations. The combination which gives the largest  $\delta_{mp}$  is recorded along with the associated solution  $E^{ps}$ ,  $Y^{ps}$ ,  $n^{ps}$  for that particular combination.

**Step 5:** Finally, determine the differences (expressed in percentage) between the true and perturbed elastic modulus, yield strength and strain hardening exponent. These percentage differences illustrate how much the material properties can deviate for a given uncertainty in the experimental measurements of the shape functions.

In the next section, the sensitivity analysis discussed above will be applied to some specific dual indentation techniques.

## 6. Sensitivity of dual indentation techniques

To elucidate the sensitivity to experimental errors for dual indentation testing, we investigate a material with elastic modulus  $E^{ts} = 180$  GPa, yield strength  $Y^{ts} = 300$  MPa and strain hardening exponent  $n^{ts} = 0.25$ , based on the procedure presented in Section 5.

### 6.1. Dual conical indentation ( $\alpha_1 = 50^\circ$ , $\alpha_2 = 80^\circ$ )

First, we apply the sensitivity analysis (Section 5) on three shape functions combinations (see Table 4) spanning a range of condition numbers: (i) ( $W_e^2, S_u^1, W_e^1$ ),  $\kappa_m^{avg} = 5.8248$ ; (ii) ( $h_f^2, S_u^1, W_e^1$ ),  $\kappa_m^{avg} = 42.715$ ; and (iii) ( $h_f^2, W_t^1, P_m^1$ ),  $\kappa_m^{avg} = 322.06$ .

The results obtained by the sensitivity analysis for the shape function combination ( $W_e^2, S_u^1, W_e^1$ ) are tabulated in Table 6, where the (unperturbed) reverse analysis results are included for comparison. For small experimental error (perturbations of  $\pm 1\%$ ), this dual indentation method predicts the material properties quite well. However, for larger experimental error, the determined material may not be reliable. For example, the material properties are more than 40% off for the error combination of  $(-5, 2.5, 5)$ . The One Factor and Uniform Factors schemes do not predict as large a deviation in material properties as that predicted by the Monte Carlo sensitivity analysis procedure. Thus, this confirms that these two schemes are not sufficient to adequately conduct a sensitivity analysis. It is interesting to note that the Monte Carlo error range of  $(-5, 2.5, 5)$  gives larger error than the cases  $(10, 10, 10)$  or  $(-10, -10, -10)$ .

Next, we consider the results that are obtained by applying the Monte Carlo sensitivity analysis on the shape function combinations with larger condition numbers, ( $h_f^2, S_u^1, W_e^1$ ),  $\kappa_m^{avg} = 42.715$  and ( $h_f^2, W_t^1, P_m^1$ ),  $\kappa_m^{avg} = 322.06$ , Table 7. Without any perturbations imposed on the shape functions, the dual indentation technique can determine material properties quite accurately using the combination ( $h_f^2, S_u^1, W_e^1$ ). However, a small error in experimental measurement can create large errors in the determined material properties. For the combination ( $h_f^2, W_t^1, P_m^1$ ), even when exact values of the shape functions are used, the deviations in material properties are very large. Thus, this is not a suitable dual indentation technique as suggested by large  $\kappa_m^{avg}$ .

From these examples, the correlation between the condition number and Monte Carlo sensitivity analysis can be seen clearly. For the three shape function combinations considered, as the condition number increases, the sensitivity to experimental errors increases.<sup>3</sup>

### 6.2. Sensitivity behavior across material range

It was discussed in Section 4 that the condition number of a dual indentation technique depends on the material being considered. Thus, the sensitivity of a dual indentation technique also depends on the material properties. Based on our investigation of various dual indentation techniques, dual indentation with

<sup>3</sup> Although, the conclusions regarding the correlation between the condition number and Monte Carlo analysis presented in this section are based on one particular material, similar conclusions are observed for a range of materials. The results for those materials are not presented for brevity.

**Table 8**

Errors in calculated material properties based on Monte Carlo sensitivity analyse for 9 selected materials spanning the  $E/Y-n$  space for dual indentation with  $\alpha_1 = 50^\circ$  and  $\alpha_2 = 80^\circ$  and shape function combination ( $W_e^1, S_u^1, W_e^1$ ).

Material Properties				Error case	Percentage error in		
$E$ (GPa)	$Y$ (MPa)	$E/Y$	$n$		$E$	$Y$	$n$
180	1200	150	0.45	(-5, 5, -5)	-1.59	38.9	-18.8
180	360	500	0.45	(-5, 5, -5)	-20.6	-74.6	9.90
180	189	950	0.45	(5, -5, 5)	-13.3	-38.9	3.69
180	1200	150	0.25	(-5, 5, -5)	-4.92	24.4	-33.4
180	360	500	0.25	(5, -5, 5)	5.99	22.9	-19.7
180	189	950	0.25	(-5, 5, 5)	6.34	24.5	-17.7
180	1200	150	0.05	(5, -5, 5)	-3.82	-91.1	674.0
180	360	500	0.05	(-5, 5, -5)	5.44	-57.8	421.0
180	189	950	0.05	(5, 2.5, -5)	6.27	19.7	-93.2

$\alpha_1 = 50^\circ$  and  $\alpha_2 = 80^\circ$  and shape function combination ( $W_e^2, S_u^1, W_e^1$ )—was found to be least sensitive to experimental errors. To investigate the effectiveness of this dual indentation technique over a range of materials, the Monte Carlo sensitivity analysis ( $\pm 5\%$  error range) has been applied to this technique for nine (9) materials, which are situated in a rectangular grid of the  $E/Y - n$  space considered (see Table 8). The results summarized in Table 8 shows that for all of the materials combinations considered, errors of at least 15% in the determined properties were obtained for at least one material property. This is quite remarkable: Even the best dual indentation technique (the technique with the lowest condition number) cannot reliably establish the material properties for a range of materials.

### 6.3. Sensitivity due to local material property variation

Dual indentation tests are typically conducted by indenting two different locations of the same specimen. Thus, in addition to errors in the experimental measurements, variations due to local material property within a specimen also affect the evaluated material properties. To explore this, two cases were considered for dual indentation with  $\alpha_1 = 50^\circ$  and  $\alpha_2 = 80^\circ$  and shape function combination resulting in the lowest condition number ( $W_e^2, S_u^1, W_e^1$ ). For indentation by indenter with  $\alpha_1 = 50^\circ$ , the original material properties were assumed as: elastic modulus,  $E^{ts} = 180$  GPa, yield strength,  $Y^{ts} = 300$  MPa and strain hardening exponent,  $n^{ts} = 0.25$ . For indentation with  $\alpha_2 = 80^\circ$ , two cases were considered: the three material parameters were (i) increased by 3% and (ii) decreased by 3%. Based on this data scatter, a Monte Carlo sensitivity analysis with error range of  $\pm 1\%$  were conducted and tabulated in Table 9. In both cases, the errors have been computed with respect to the nominal values ( $E^{ts} = 180$  GPa,  $Y^{ts} = 300$  MPa and  $n^{ts} = 0.25$ ). The results show that even for small experimental error (perturbations of  $\pm 1\%$ ), the error in the determined material properties can be in the order of 20%.

### 6.4. A note on the use of condition number vs sensitivity analysis

As discussed previously, the condition number provides guidelines about the effectiveness of an indentation technique whereas the sensitivity analysis provides numerical estimates of possible errors in the determined material properties. However, a sensitivity analysis is significantly more computationally intense to perform than computing a condition number: it takes a CPU time of about 2 s to compute the condition number for a material using the computational procedure outlined in Section 4.2, whereas a typical Monte Carlo sensitivity analysis takes about 50 min using the steps outlined in Section 5. Calculations were performed using a DELL OptiPlex 990 Desktop computer with Intel(R) Core(TM) i5-

**Table 9**

Errors in calculated material properties based on Monte Carlo sensitivity analysis for dual indentation with  $\alpha_1 = 50^\circ$  and  $\alpha_2 = 80^\circ$  and shape function combination ( $W_e^2, S_u^1, W_e^1$ ), to investigate the effect of local material property variation.

Material Properties	Percentage error in determined material properties			
	Material properties increased by 3% for $\alpha_2 = 80^\circ$		Material properties decreased by 3% for $\alpha_2 = 80^\circ$	
	0%	$\pm 1\%$ (1, 1, -1)	0%	$\pm 1\%$ (-1, -1, 1)
$E$	0.750	2.05	-0.914	-2.15
$Y$	-14.9	-18.2	16.2	20.1
$n$	11.71	15.2	-12.2	-15.7

2500 processor. Thus, determining the condition number first will serve as a useful guidance in selecting data reduction schemes.

## 7. Concluding remarks

This work explored the uniqueness and sensitivity to experimental errors when evaluating instrumented indentation. Of particular interests is to extract the elastic modulus, the yield strength and strain hardening coefficient of homogeneous, isotropic material with linear-elastic and power-law strain hardening plasticity. To this end, a systematic investigation considering the concept of condition numbers, along with explicit numerical approaches for characterizing the sensitivity to experimental errors was carried out. The methods investigated are all based on considering “shape functions,” which are sets of functions that describe the force–displacement relationship obtained during the indentation testing.

We extend the definition of condition numbers, and explore its use for dual indentation testing. In its redefined form, condition numbers and iso- $(P_m/S_u h_m)$  lines provide a comprehensive quantitative description characterizing uniqueness and sensitivity for indentation techniques. When considering condition number and the iso- $(P_m/S_u h_m)$  lines, it is clear that non-uniqueness is an extreme case of sensitivity for experimental errors. In particular, we show that the reliability of a dual indentation technique highly depends on the selection of the three shape functions that are needed to determine the three unknown material properties.

Condition numbers are useful in determining effective choices of two half-angle combinations that reduce sensitivity to experimental error when utilizing dual indentation techniques. However, as a complement to the condition numbers, numerical sensitivity analyses reveal more insight. To this end, three approaches for conducting numerical sensitivity analysis were investigated. A procedure based on a Monte Carlo approach was found to be more effective than both the One Factor (shape functions varied one at a time) and the Uniform Factors (all shape functions increased or decreased by same amount) schemes. The Monte Carlo sensitivity analysis procedure was applied to a wide range of dual indentation techniques with,  $50^\circ \leq \alpha \leq 80^\circ$ . The most effective (least sensitive) conical dual indentation technique was suggested to be indentation with  $\alpha_1 = 50^\circ$  and  $\alpha_2 = 80^\circ$  and shape function combination (elastic energy,  $W_e$  and unloading slope,  $S_u$  from  $\alpha_1 = 50^\circ$ ; elastic energy,  $W_e$  from  $\alpha_2 = 80^\circ$ ), which is consistent with having the lowest condition number.

Based on the Monte Carlo sensitivity analysis we conclude that dual indentation techniques are reliable when the experimental error is within  $\pm 1\%$ . However, for the error range of  $\pm 5\%$ , none of the three material properties can be determined with reasonable reliability. Moreover, when considering that local material property may vary between the two indentations, the effectiveness of the dual indentation technique may be questionable. New dual inden-

tation techniques need to be developed to overcome the problem of sensitivity to experimental error.

## Appendix A

The condition number can be used to quantify the sensitivity of a system (Datta, 2010). Generally, the condition number gives a measure of the ratio of error in the solution to the error in the data. For a system with a large condition number, a small perturbation in the data will cause a large error in the solution. Thus, a system with a large condition number is sensitive to experimental errors; an ill conditioned system. A small condition number implies that the system is not sensitive to perturbations (experimental errors); a well-conditioned system. The condition number is an inherent property of the problem and does not depend on the algorithm that is used to solve the system.

Consider the general system (linear or nonlinear) of equations,  $\mathbf{f}(\mathbf{x}) = \mathbf{y}$ , where  $\mathbf{x}$  is the input/solution vector (e.g. the material parameters set  $(E, Y, n)$ ) and  $\mathbf{y}$  the output/data vector (e.g. the set of shape functions). Assuming that the solution of the system  $\mathbf{f}(\mathbf{x}) = \mathbf{y}$  exists, the aim of the sensitivity analysis is to investigate how a small perturbation,  $\Delta\mathbf{y}$ , of the output vector causes a changes the input vector,  $\Delta\mathbf{x}$ . With the perturbations, the system of equations can be written as  $\mathbf{f}(\mathbf{x} + \Delta\mathbf{x}) = \mathbf{y} + \Delta\mathbf{y}$ . For the special case of a linear system, the system of equation,  $\mathbf{f}(\mathbf{x}) = \mathbf{y}$  can be expressed as  $\mathbf{A}\mathbf{x} = \mathbf{y}$ , where  $\mathbf{A}$  is a matrix, and  $\mathbf{x}$  and  $\mathbf{y}$  are vectors. Hence,  $\mathbf{A}(\mathbf{x} + \Delta\mathbf{x}) = \mathbf{y} + \Delta\mathbf{y}$ .

There are two definitions of condition numbers (Higham, 1996; Rheinboldt, 1976). One relates to the absolute error in data or solution, and the other to the relative error. The second condition number is used more widely than the first condition number, since the relative error tends to be more useful than the absolute error. For a general system,  $\mathbf{f}(\mathbf{x}) = \mathbf{y}$ , the second condition number at a point  $\mathbf{z}$ , of the domain (of  $\mathbf{x}$ ), is given by:

$$\kappa = v(\mathbf{f}, C, \mathbf{z})/u(\mathbf{f}, C, \mathbf{z}) \quad (\text{A1a})$$

where

$$v(\mathbf{f}, C, \mathbf{z}) = \inf_{\mathbf{x} \text{ in } C} \{t \text{ in } [0, \infty); \|\mathbf{f}(\mathbf{x}) - \mathbf{f}(\mathbf{z})\| \leq t\|\mathbf{x} - \mathbf{z}\|\} \\ u(\mathbf{f}, C, \mathbf{z}) = \sup_{\mathbf{x} \text{ in } C} \{t \text{ in } [0, \infty); \|\mathbf{f}(\mathbf{x}) - \mathbf{f}(\mathbf{z})\| \geq t\|\mathbf{x} - \mathbf{z}\|\} \quad (\text{A1b})$$

Here,  $C$  is a sub-domain enclosing the point  $\mathbf{z}$ ,  $\|\cdot\|$  denotes the norm of the vector, which is defined as (for vector  $\mathbf{z}$ ):

$$\|\mathbf{z}\|_p = \left( \sum_{i=1}^n |z_i|^p \right)^{1/p} \quad (\text{A2})$$

where  $p \geq 1$  and is a real number. Different norms can be defined depending on the values of  $p$ . The most commonly used norm, the Euclidean norm ( $p=2$ ) is used here. For the linear system, the second condition number reduces to a simpler expression, which is given as follows:

$$\kappa = \|\mathbf{A}\| \|\mathbf{A}^{-1}\| \quad (\text{A3})$$

It can be shown that, small a  $\kappa$  implies that  $\|\Delta\mathbf{x}\|/\|\mathbf{x}\|$  is small for a given  $\|\Delta\mathbf{y}\|/\|\mathbf{y}\|$  and vice versa.

To illustrate how the condition number can quantify the sensitivity of a system, we considered four simple 2 by 2 linear systems. The condition numbers (Eq. (A1)) for these systems are tabulated in Table A1. For each of the four examples considered, the original system was perturbed by changing the first element of the data vector,  $\mathbf{y}$ , by 1%. The solutions of the original and perturbed systems were computed and percentage differences were determined. It can be seen from Table A1 that the error increases with condition number increasing. The fourth example is of a non-unique system for which the condition number is infinity. Fig. A1 provides a graphical representation of the four systems. It can be seen that, as the condition number of the system increases, the straight lines get closer to each other. For the third example, the straight lines are so close that it appears they have overlapped. Finally, in the fourth example, when the two straight lines actually overlap, the solution becomes non-unique (figure omitted due to its triviality). Thus, non-uniqueness can be considered as an extreme case of highly sensitive system.

## Appendix B

In order to carry out the sensitivity analyse outlined in Section 5, one needs to solve the functional equations to obtain the material properties. Denoting the three selected shape functions to be  $\mathfrak{S}_1, \mathfrak{S}_2$  and  $\mathfrak{S}_3$ , the three equations to be solved are:

$$\mathfrak{S}_i = \Theta_i(E, Y, n); \quad i = 1, 2, 3 \quad (\text{B1})$$

In this set of equations, the quantities on the left hand side (the three shape functions), and the functions  $\Theta_1, \Theta_2$  and  $\Theta_3$  are known. The material properties  $E, Y$  and  $n$  need to be determined. The functions  $\Theta_1, \Theta_2$  and  $\Theta_3$  are highly nonlinear fitting functions (see Section 2.2). Non-linear system can be solved numerically using an iterative process. The predicted material properties,  $E^{pr}, Y^{pr}$  and  $n^{pr}$ , is the set for which the residual (or the distance) between the vectors  $(\mathfrak{S}_1, \mathfrak{S}_2, \mathfrak{S}_3)$  and  $(\Theta_1(E^{pr}, Y^{pr}, n^{pr}), \Theta_2(E^{pr}, Y^{pr}, n^{pr}), \Theta_3(E^{pr}, Y^{pr}, n^{pr}))$  is minimized according to

$$\delta_{sf} = \sqrt{\left(\frac{sf_1 - f_1}{sf_1}\right)^2 + \left(\frac{sf_2 - f_2}{sf_2}\right)^2 + \left(\frac{sf_3 - f_3}{sf_3}\right)^2} \quad (\text{B2})$$

The ordinary line search and golden section line search (Arora, 2012) methods were impractical to use for solving the present nonlinear system because of very high computational cost involved. Although the Newton-Raphson method (Arora, 2012) converged much faster, the convergence is dependent on the initial guess. Further, the Newton-Raphson method works well for a well-posed system, but does not converge for an ill-posed system. Thus, we use, a combination of the three methods to solve the set

**Table A1**  
Correlation between condition number and the sensitivity to perturbation in four linear systems.

Example	Original system ( $Ax = y$ )	Perturbed system	Condition number (of A)	Solution of the original system	Solution of the Perturbed system	Percentage change in the solution
a	$\begin{bmatrix} 1 & 3 \\ 5 & -1 \end{bmatrix} \begin{bmatrix} x_1 \\ x_2 \end{bmatrix} = \begin{bmatrix} 4 \\ 4 \end{bmatrix}$	$\begin{bmatrix} 1 & 3 \\ 5 & -1 \end{bmatrix} \begin{bmatrix} x_1 \\ x_2 \end{bmatrix} = \begin{bmatrix} 4.04 \\ 4 \end{bmatrix}$	1.6400	$x_1 = 1$ $x_2 = 1$	$x_1 = 1.0025$ $x_2 = 1.0125$	$x_1: 0.25$ $x_2: 1.25$
b	$\begin{bmatrix} 1 & 3 \\ 5 & 6 \end{bmatrix} \begin{bmatrix} x_1 \\ x_2 \end{bmatrix} = \begin{bmatrix} 4 \\ 11 \end{bmatrix}$	$\begin{bmatrix} 1 & 3 \\ 5 & 6 \end{bmatrix} \begin{bmatrix} x_1 \\ x_2 \end{bmatrix} = \begin{bmatrix} 4.04 \\ 11 \end{bmatrix}$	7.7606	$x_1 = 1$ $x_2 = 1$	$x_1 = 0.9733$ $x_2 = 1.0222$	$x_1: 2.67$ $x_2: 2.22$
c	$\begin{bmatrix} 1000 & 999 \\ 999 & 998 \end{bmatrix} \begin{bmatrix} x_1 \\ x_2 \end{bmatrix} = \begin{bmatrix} 1999 \\ 1997 \end{bmatrix}$	$\begin{bmatrix} 1000 & 999 \\ 999 & 998 \end{bmatrix} \begin{bmatrix} x_1 \\ x_2 \end{bmatrix} = \begin{bmatrix} 2019 \\ 1997 \end{bmatrix}$	3.99E6	$x_1 = 1$ $x_2 = 1$	$x_1 = -1.995E4$ $x_2 = 1.997E4$	$x_1: 1.995E6$ $x_2: -1.997E6$
d	$\begin{bmatrix} 5 & 6 \\ 5 & 6 \end{bmatrix} \begin{bmatrix} x_1 \\ x_2 \end{bmatrix} = \begin{bmatrix} 11 \\ 11 \end{bmatrix}$	-	Infinity	Non-unique	-	-

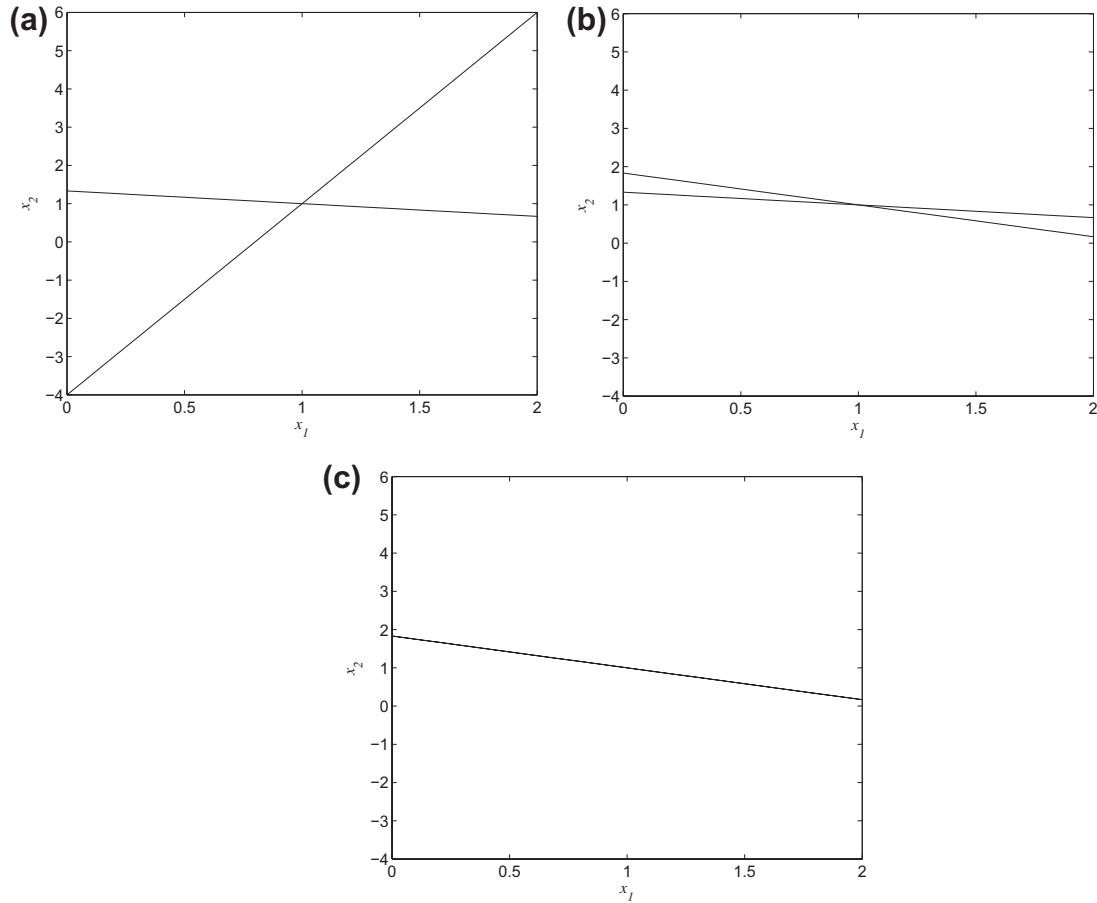


**Fig. A1.** Three systems of straight lines (examples a–c of Table 1) with increasing condition number and sensitivity. As the condition number increases, the straight lines approach each other and finally overlap.

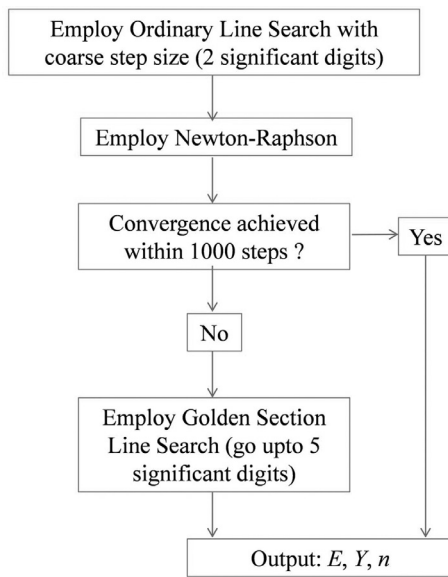


**Fig. B1.** Algorithm used to solve the nonlinear set of equations.

of nonlinear equations in the present work. The algorithm is schematically shown in Fig. B1. At first, an ordinary line search is employed to determine the solution. The predicted solution is fed as an initial guess to a Newton–Raphson algorithm. If the solution

converges, the algorithm is ended. If it does not converge after 1000 Newton–Raphson iterations, a golden section line search is employed thereafter starting from the solution of the ordinary line search.

## References

- Alkorta, J., Martínez-Esnaola, J.M., Sevillano, J.G., 2005. Absence of one-to-one correspondence between elastoplastic properties and sharp-indentation load-penetration data. *J. Mater. Res.* 20, 432–437.
- Arora, J., 2012. *Introduction to Optimum Design*. Elsevier.
- Bowden, F.P., Tabor, D., 2001. *The Friction and Lubrication of Solids*. Oxford University Press.
- Bucaille, J.L., Stauss, S., Felder, E., Michler, J., 2003. Determination of plastic properties of metals by instrumented indentation using different sharp indenters. *Acta Mater.* 51, 1663–1678.
- Buckingham, E., 1914. On physically similar systems; illustrations of the use of dimensional equations. *Phys. Rev.* 4, 345–376.
- Cao, Y., Huber, N., 2006. Further investigation on the definition of the representative strain in conical indentation. *J. Mater. Res.* 21, 1810–1821.
- Cao, Y.P., Lu, J., 2004a. A new method to extract the plastic properties of metal materials from an instrumented spherical indentation loading curve. *Acta Mater.* 52, 4023–4032.
- Cao, Y.P., Lu, J., 2004b. Depth-sensing instrumented indentation with dual sharp indenters: stability analysis and corresponding regularization schemes. *Acta Mater.* 52, 1143–1153.
- Cao, Y.P., Qian, X.Q., Lu, J., Yao, Z.H., 2005. An energy-based method to extract plastic properties of metal materials from conical indentation tests. *J. Mater. Res.* 20, 1194–1206.
- Capehart, T.W., Cheng, Y.-T., 2003. Determining constitutive models from conical indentation: sensitivity analysis. *J. Mater. Res.* 18, 827–832.
- Chen, X., Ogasawara, N., Zhao, M., Chiba, N., 2007. On the uniqueness of measuring elastoplastic properties from indentation: the indistinguishable mystical materials. *J. Mech. Phys. Solids* 55, 1618–1660.

- Cheng, Y.-T., Cheng, C.-M., 1999. Can stress-strain relationships be obtained from indentation curves using conical and pyramidal indenters? *J. Mater. Res.* 14, 3493–3496.
- Cheng, Y.T., Cheng, C.M., 2004. Scaling, dimensional analysis, and indentation measurements. *Mater. Sci. Eng. R* 44, 91–149.
- Chollacoop, N., Dao, M., Suresh, S., 2003. Depth-sensing instrumented indentation with dual sharp indenters. *Acta Mater.* 51, 3713–3729.
- Dao, M., Lim, C., Suresh, S., 2003. Mechanics of the human red blood cell deformed by optical tweezers. *J. Mech. Phys. Solids* 51, 2259–2280.
- Datta, B.N., 2010. *Numerical Linear Algebra and Applications*. Society for Industrial and Applied Mathematics.
- Dieter, G., 1976. *Mechanical Metallurgy*, second ed. McGraw-Hill, New York.
- Heinrich, C., Waas, A.M., Wineman, A.S., 2009. Determination of material properties using nanoindentation and multiple indenter tips. *Int. J. Solids Struct.* 46, 364–376.
- Higham, N.J., 1996. *Accuracy and stability of numerical algorithms*. Society for Industrial and Applied Mathematics.
- Hyun, H.C., Kim, M., Lee, J.H., Lee, H., 2011. A dual conical indentation technique based on FEA solutions for property evaluation. *Mech. Mater.* 43, 313–331.
- Johnson, K.L., 1987. *Contact Mechanics*. Cambridge University Press.
- Huang, Y., Zhang, F., Hwang, K.C., Nix, W.D., Pharr, G.M., Feng, G., 2006. A model of size effects in nano-indentation. *J. Mech. Phys. Solids* 54, 1668–1686.
- Kim, J.-Y., Kang, S.-K., Lee, J.-J., Jang, J.-I., Lee, Y.-H., Kwon, D., 2007. Influence of surface-roughness on indentation size effect. *Acta Mater.* 55, 3555–3562.
- Lan, H., Venkatesh, T.A., 2007. Determination of the elastic and plastic properties of materials through instrumented indentation with reduced sensitivity. *Acta Mater.* 55, 2025–2041.
- Le, M.-Q., 2008. A computational study on the instrumented sharp indentations with dual indenters. *Int. J. Solids Struct.* 45, 2818–2835.
- Le, M.-Q., 2009. Material characterization by dual sharp indenters. *Int. J. Solids Struct.* 46, 2988–2998.
- Le, M.-Q., 2011. Improved reverse analysis for material characterization with dual sharp indenters. *Int. J. Solids Struct.* 48, 1600–1609.
- Lichinchi, M., Lenardi, C., Haupt, J., Vitali, R., 1998. Simulation of Berkovich nanoindentation experiments on thin films using finite element method. *Thin Solid Films* 312, 240–248.
- Lubliner, J., 1990. *Plasticity Theory*. Macmillan, New York.
- Ogasawara, N., Chiba, N., Chen, X., 2009. A simple framework of spherical indentation for measuring elastoplastic properties. *Mech. Mater.* 41, 1025–1033.
- Oliver, W.C., Pharr, G.M., 1992. An improved technique for determining hardness and elastic modulus using load and displacement sensing indentation experiments. *J. Mater. Res.* 7, 1564–1583.
- Rheinboldt, W.C., 1976. On measures of ill-conditioning for nonlinear equations. *Math. Comput.* 30, 104–111.
- Swaddiwudhipong, S., Tho, K.K., Liu, Z.S., Zeng, K., 2005. Material characterization based on dual indenters. *Int. J. Solids Struct.* 42, 69–83.
- Tho, K.K., Swaddiwudhipong, S., Liu, Z.S., Zeng, K., Hua, J., 2004. Uniqueness of reverse analysis from conical indentation tests. *J. Mater. Res.* 19, 2498–2502.
- Wang, L., Ganor, M., Rokhlin, S.I., 2005. Inverse scaling functions in nanoindentation with sharp indenters: determination of material properties. *J. Mater. Res.* 20, 987–1001.
- Yan, J., Chen, X., Karlsson, A., 2007a. Determining equi-biaxial residual stress and mechanical properties from the force-displacement curves of conical microindentation. *J. Eng. Mater. Technol.* 129, 200.
- Yan, J., Karlsson, A., Chen, X., 2007b. Determining plastic properties of a material with residual stress by using conical indentation. *Int. J. Solids Struct.* 44, 3720–3737.